Characterization of Body Shadowing Effects on Ultra-Wideband Propagation Channel

Apichit Pradubphon*, Sathaporn Promwong*,**, Monchai Chamchoy*,
Pichaya Supanakoon*, and Jun-ichi Takada**

*Department of Information Engineering, Faculty of Engineering,
King Mongkut's Institute of Technology Ladkrabang
Chalongkrung Rd., Ladkrabang, Bangkok 10520, Thailand
Tel: +66 2 7372500-47 Ext. 5140 Fax: +66 2 3264176
E-mail: {s6064613,kcmoncha,kspichay}@kmitl.ac.th
**Graduate School of Science and Engineering,
Tokyo Institute of Technology
2-12-1, O-okayama, Meguro-ku, Tokyo 152-8552, Japan
E-mail: ken@ap.ide.titech.ac.jp

Abstract: There are several factors that disturb an Ultra-Wideband (UWB) radio propagation in an indoor environment such as path loss, shadowing and multipath fading. These factors directly affect the quality of the received signal. In this paper, we investigated the influence of the human body shadowing on UWB propagation based on measured wireless channel in an anechoic chamber. The characteristics of the UWB channel including the transmitter and the receiver antenna effects are acquired over the frequency bandwidth of 3∼11 GHz. The major factors such as the power delay profile (PDP), the angular power distribution (APD), the pulse distortion and the RMS delay spread caused by the human body shadowing are presented.

Keywords: Ultra-wideband communication, body shadowing, delay spread, pulse distortion

1. Introduction

Recently, the ultra wideband (UWB) radio technology is becoming an interesting topic for the wireless communication. The UWB system is different from other radio communication technology. Instead of using narrow carrier frequency, the UWB transmits the pulse of power which is in the range of ultra-wide frequency spectrum. The US Federal Communication Commission (FCC) specifies that the UWB signal has the frequency spectrum range from 3.1 GHz to 10.6 GHz [1]. The UWB technology is an ideal candidate that can be utilized for commercial, short-range, low power, and low cost indoor communication systems such as Wireless Personal Area Networks (WPANs) [2], [3]. Hence, the characterization of an indoor radio channel is very important if we will use this technology in the realworld. Also, the effect of human body shadowing affecting to the signal level in the received part are also considered. Research about the influence of the human body on the radio channel has been in progress for several literatures [4]-[6]. A recent example of such a research by Welch *et al.* [4] which detailed the characteristic of the UWB antenna using traditional anechoic-chamber measurement techniques and characterize the power pattern of the UWB antenna with as the human body obstacte in the indoor environment. The RF environment is relatively quiet in the frequency range of interest (1-3 GHz)., Sanchez *et al.*[5]detailed their analytical results of human operator effect on the wideband and narrowband channel and Zasowski *et al.* [6] detailed their UWB channel measurements from 3∼6 GHz for a body area network (BAN) in the anechoic chamber and an office room. But these researches do not consider the influence of the human body shadowing on the UWB communication channel by statistical process such as the mean excess delay, the RMS delay spread etc. are also an important parameter.

In this paper, we investigated the influence of the human body showing on the UWB propagation over the frequency bandwidth of 3∼11 GHz. The experimental channels are taken in the anechoic chamber to avoid the environmental effects. However, the characteristics of the transmitter and receiver antennas are included in the channel. In the experiment, a handmade biconical antenna and the commercial, small-size, low profile antenna developed by Skycross, are used at the transmitter and receiver, respectively. From the experimental results, the channel parameters such as the power delay profile, the RMS delay spread, the correlation coefficient and the angular power distribution are seen directly to be affected by the human body shadowing.

2. Investigation Parameters

2.1. Time Dispersion

In order to investigate the effects of the human body shadowing, we considered the time delay of the arrived signal at the receiver. Multiple reflections of the transmitted signal may arrive at the receiver at different times, resulting in intersymbol interference (ISI, or bits into one another) which the receiver cannot sort out. The time dispersion can be analyzed by using the mean excess delay, τ_m, and the RMS delay spread, τ_{rms}, to illustrate the effects of body shadowing. The mean excess delay which is the first central moment of $|h(t)|^2$ and the RMS delay spread which is the square root of the second central moment of $|h(t)|^2$ take into account the relative powers of the taps as well as their delays, making it a better indicator of system performance than the other parameters. The mean excess delay, τ_m, is defined as [6]

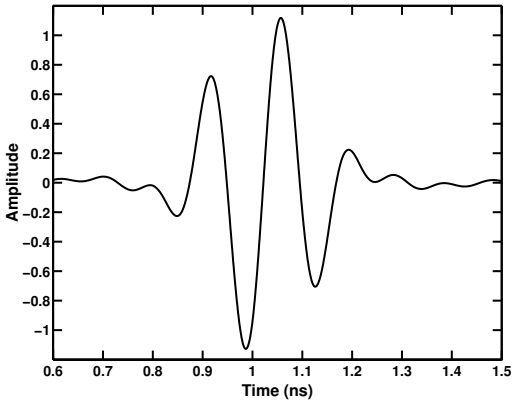

Fig. 1. The transmitted UWB signal waveform.

$$\tau_m = \frac{\int_0^\infty \tau \cdot |h(\tau)|^2 d\tau}{\int_0^\infty |h(\tau)|^2 d\tau}, \tag{1}$$

and the RMS delay spread, τ_{rms}, can be defined by

$$\tau_{rms} = \sqrt{\frac{\int_0^\infty (\tau - \tau_m)^2 \cdot |h(\tau)|^2 d\tau}{\int_0^\infty |h(\tau)|^2 d\tau}}. \tag{2}$$

2.2. Pulse Distortion

The pulse distortion is the changing effect of the signal (shape) when the signal is transmitted to the receiver side. This factor shows the performance of the matched filter at the receiver side to maximize the SNR for evaluation in the UWB system. For the distortion quantity of the pulse waveform, we will consider the correlation coefficient, $\rho_{(d)}$, of the transmitted and received pulse waveform at an arbitrary angle. The correlation coefficient is defined by

$$\rho_{(d)} = \frac{\max |r_{ab}(\tau)|}{\max |\sqrt{r_a(\tau) r_b(\tau)}|}, \tag{3}$$

where $r_{ab}(\tau)$ is the cross-correlation of two signals describing the general dependence of one signal with respect to the other, while the time lag(t) is varied and T is the time period. The cross-correlation function, $r_{ab}(\tau)$, is defined as [7]

$$\begin{aligned} R_{xy}(\tau) &= x(t)y(t-\tau) \\ &= \lim_{T\to\infty} \frac{1}{T} \int_{-\infty}^{\infty} x(t)y(t+\tau)dt, \end{aligned} \tag{4}$$

which $r_a(\tau)$ and $r_b(\tau)$ are the auto-correlation functions and can be written as

$$\begin{aligned} R_x(\tau) &= E[x_k(t)x_k(t+\tau)] \\ &= \lim_{T\to\infty} \frac{1}{T} \int_{-\infty}^{\infty} x(t)x(t+\tau)dt. \end{aligned} \tag{5}$$

3. Description of Measurement

3.1. UWB Signal Model

In order to investigate the pulse distortion, the UWB signal model for transmitted pulse is required. We considered the impulse radio signal which fully covers the FCC band [1], 3.1∼10.6 GHz. The center frequency and the total bandwidth were, therefore, set to be $f_0 = 6.85$ GHz and $f_b = 7.5$ GHz, respectively. The transmitted waveform assumed in the simulation is a single ASK pulse with the carrier frequency f_0. The parameter t_0 is set to be $7/f_0$. To satisfy the bandwidth requirement of f_b, the pulse length was set to be $2/f_b$ (t_d). Then, the signal is band-limited by a Nyquist roll-off filter with roll-off factor of 0 (rectangular window) and passband $(f_0\text{-}\frac{f_b}{2}, f_0\text{+}\frac{f_b}{2})$. These UWB pulses are normalized by coefficient v_0 to have the energy of 1 J. Fig. 1 shows the transmitted pulse waveform and its equation is

$$v_t(t) = v_0 \exp^{-[(t-t_0)/(t_d/2)]^2} \sin(2\pi f_0 t). \tag{6}$$

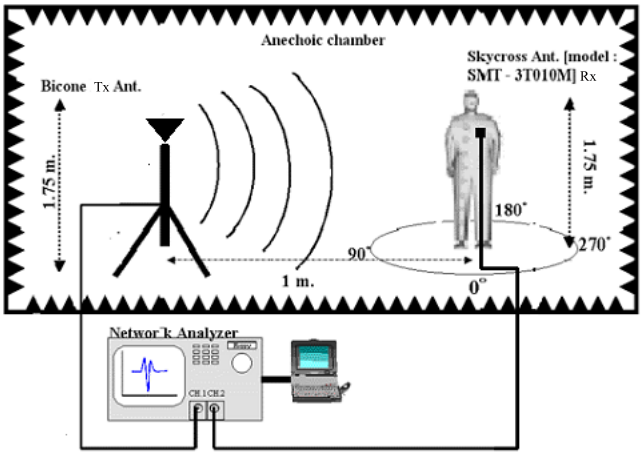

Fig. 2. The measurement setup.

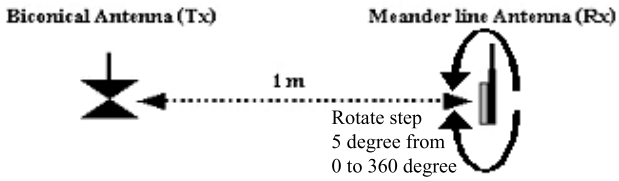

Fig. 3. Top view antenna setting.

3.2. Measurement Setup

The UWB radio channel transfer function is measured as S_{21} in the frequency domain by using a vector network analyzer (VNA) operated in the response measurement mode, where Port-1 is the transmitter port (TX) and Port-2 is the receiver port (RX). The handmade biconical antenna and the commercial, small-size, low profile antenna developed by Skycross Lnc.,(USA) [8] are used at the transmitter and the receiver, respectively. The biconical antenna with maximum diameter of 65.3 mm and length of 37 mm is used as the transmitted antenna [9]. Both antennas are placed at a height of 1.75 m and separation distance of 1 m. The receiver antenna is placed near the human body. For each measured channel, the antenna is rotated in an increment of 5° from 0° to 360° while recording the received power. The measurement is carried out in an anechoic chamber.The setup

is sketched for the measurement setup and the top view antenna are shown in Fig. 2 and Fig. 3, respectively.

3.3. Experiment Parameters

The important parameters for the experiments are listed in Table 1. It is noted that the calibration is done at the connectors of the cables to be connected to the antennas. Therefore, all the impairments of the antenna characteristics are included in the measured results. The dynamic range mentioned in Table.1 is reduced to the output of the RX antenna. Specified dynamic range for the network analyzer is 100 dB but the cable losses snip some 20 dB of the dynamic range. The number of frequency point over the band is set to 1601, the frequency resolution is 5 MHz per point and the time resolution is 0.2 μ_s.

3.4. Signal Processing and Data Analysis

The impulse response of the channel is obtained by performing the IDFT on the frequency response of the channel. The frequency domain data is first filtered using a Hamming window prior to performing the IDFT. This filtering procedure reduces the side lobes of the impulse response and broadens the main lobe. Hence, the UWB channel characteristics can be analyzed statistically.

4. Experimental Results

By using the vector network analyzer, the measured frequency transfer functions with the number of frequency point of 1601 are taken in the anechoic chamber. The time domain impulse responses of the UWB channel are analyzed by the procedures described above. Figures 4 and 5 show the comparison of the power delay profile (PDP) with and without the human body shadowing at the arbitrary angle (0∼360°). From Fig. 5, we can see that the signal is attenuated by the human body shadowing between 135 and 225 degree, which is more than the other angles. For Fig. 4, the signal at angles 90 and 270 degree is did not appear because the meander-line antenna in the receiver side can not receive the signal at the left and right edges of the antenna.

The comparison of the RMS delay spread, τ_{rms}, with and without the human body shadowing at the arbitrary angle (0∼360°) is shown in Fig. 6. From the figure, we can see that the RMS delay spread of the signal between 170 and 200 degree with peak of 8 ns is more than the signal at an other angle. These results are indicated in the reduction of data rate of this system in the human body shadowing case. For the distortion quantity of the pulse waveform in the received signal shown in Fig. 7, we will consider the correlation coefficient of the transmitted UWB signal and the received signal with and without the human body shadowing. From Fig. 7, we can see that the correlation coefficient of any angle in both case, is more than 0.6. Fig. 8 shows the APD of the received signal. We can observe that the delay spread and the APD of the human body shadowing case are more than those without human body case, especially for the full shadowing at the pointing angle of 180°. The signal is attenuated by 27 dB between 170 and 190 degrees.

Table 1. Experiment parameters

Parameter	Value
Frequency range	3.0∼11.0 GHz
Number of frequency point	1601
Dynamic range	80 dB
Tx antenna height	1.75 m.
Rx antenna height	1.75 m.
Distance between Tx and Rx	1.0 m.
Pointing angle	0∼360 degrees
Rotation	5°/step

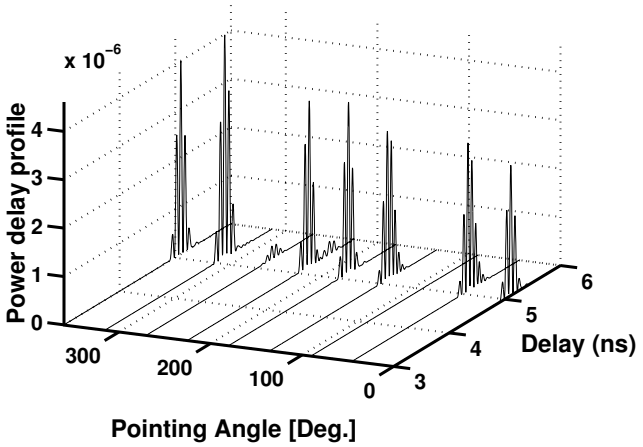

Fig. 4. The power delay profile of UWB channel without human body shadowing.

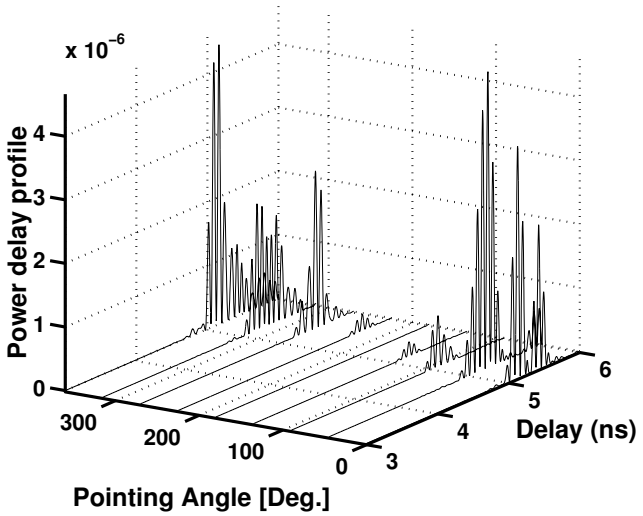

Fig. 5. The power delay profile of UWB channel with human body shadowing.

5. Conclusion

In this paper, the influence of the human body shadowing on the ultra-wideband propagation channel is investigated. As the experimental results show, we can observe that the human body shadowing directly affects the RMS delay spread, τ_{rms}, the distortion of the pulse waveform at the arbitrary

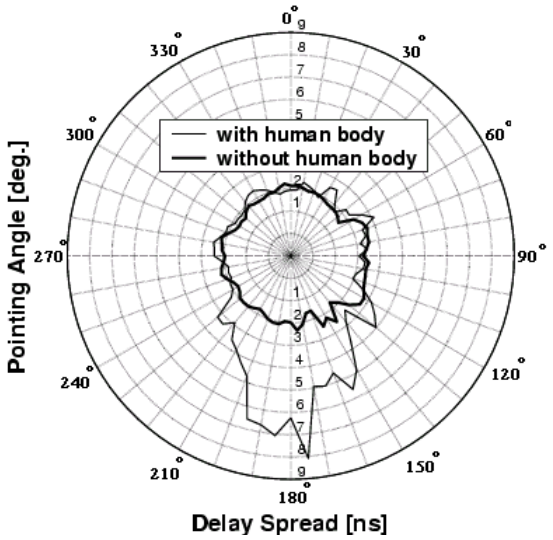

Fig. 6. The RMS delay spread, τ_{rms}, with and without human body shadowing.

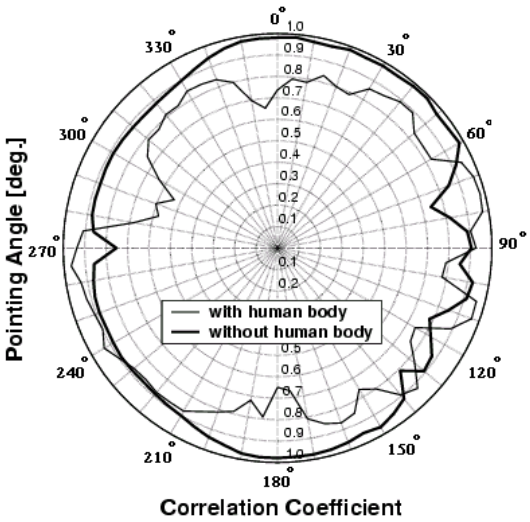

Fig. 7. The correlation between the transmitted UWB signal and the received signal, in the case of with and without the human body shadowing.

angle in the receiver side and the angular power distribution of the received signal. These measurement results indicate that while the human body creates the delay spread increased from 2 ns to 8 ns, the received signal is also attenuated by 27 dB between 170 and 190 degree which suggests that the system performance will depend greatly on the signal angle of arrival and create the distortion of the received signal (a little bit) in the case of full shadowing. Hence, the UWB communication system design must consider the influence of human body shadowing when high data transmission rates are required.

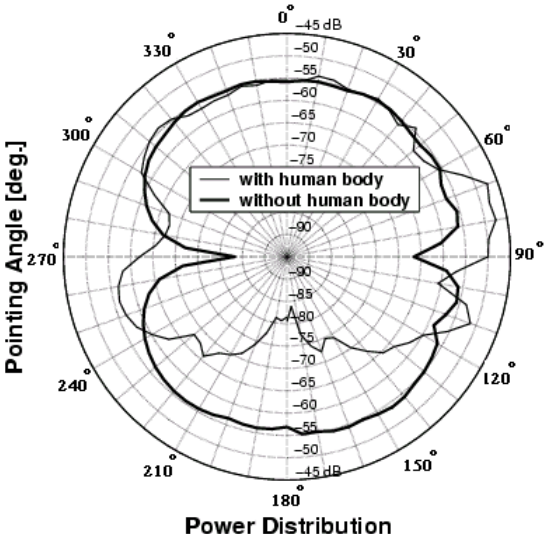

Fig. 8. The angular power distribution with and without the human body shadowing.

References

[1] Federal Communications Commission, "Revision of Part 15 of the Commission 's Rules Regarding UWB Transmission System," First Report, FCC 02-48, Apr. 2002.

[2] K. Siwiak, "Ultra-Wide Radio: Introducing a New Technology," *Proc. 2001 Spring IEEE Veh. Tech. Conf. (VTC)*, vol. 2, pp. 1088-1093, May 2001.

[3] K. Siwiak, "Ultra-Wide Radio: The emergence of an Important RF Technology," *Proc. 2001 Spring IEEE Veh. Tech. Conf. (VTC)*, vol. 2, pp. 1169-1172, May 2001.

[4] T. B. Welch, R. L. Musselman, B. A. Emessiene, P. D. Gift, D. K. Choudhury, D. N. Cassadine, and S. M. Yano, "The effects of the human body on UWB signal propagation in an indoor environment," *IEEE J. Select. Areas Commun.*, vol. 20, no. 9, pp. 1778- 1782, Dec. 2002.

[5] M. Sanchez, L. de Haro, A. Pino, and M. Calvo, "Human operator effect on wide-band radio channal characteristics," *IEEE Trans. Antennas and Propag.*, vol. 45 no. 8, pp. 1318-1320, Aug. 1997.

[6] T. Zasowski, F. Althaus, M. Stager, A. Wittneben, and G. Troster, "UWB for noninvasive wireless body area networks: Channel measurements and results," *IEEE Conf. (UWBST)*, pp. 285-289, Nov. 2003.

[7] J. D. Taylor, *Introduction to Ultra-Wideband Radar Systems*, CRC Press, Inc., 1995.

[8] Skycross, Inc., "3.1-10 GHz UWB Antenna for Commercial UWB Applications" *http://www.skycross.com/*

[9] S. Promwong, W. Hachitani, I. Ida, J. Takada, P. Supanakoon, and P. Tangtisanon, "Experimental Evaluation of Free Space Transmission Gain of UWB-IR Systems," Proceedings of The First Electrical Engineering/Electronics, Computer, Telecommunications and Information Technology (ECTI) Annual Conference, pp. 295–298, May 2004.